HHS Public Access

Author manuscript

J Cell Biochem. Author manuscript; available in PMC 2020 April 01.

Published in final edited form as:

J Cell Biochem. 2019 April ; 120(4): 6004–6014. doi:10.1002/jcb.27887.

Putative tumor suppressor cytoglobin promotes aryl hydrocarbon receptor ligand-mediated triple negative breast cancer cell death

Leah K. Rowland[1], **Petreena S. Campbell**[1], **Nicole Mavingire**[1], **Jonathan V. Wooten**[1], **Lancelot McLean**[2], **Dain Zylstra**[3], **Gabriell Thorne**[1,4], **Devin Daly**[1], **Kristopher Boyle**[3], **Sonya Whang**[1], **Juli Unternaehrer**[1], and **Eileen J. Brantley**[1,3,*]

[1]Department of Basic Sciences, Center for Health Disparities and Molecular Medicine, Loma Linda University Health School of Medicine, Loma Linda, CA

[2]Dental Education Services, Loma Linda University Health School of Dentistry, Loma Linda, CA

[3]Department of Pharmaceutical and Administrative Sciences, Loma Linda University Health School of Pharmacy, Loma Linda, CA

[4]Department of Pharmacy and Health Professions, Elizabeth City State University, Elizabeth City, NC, USA

Abstract

Nearly 40,000 women die annually from breast cancer in the US. Clinically available targeted breast cancer therapy is largely ineffective in triple negative breast cancer (TNBC), characterized by tumors that lack expression of the estrogen receptor (ER), progesterone receptor (PR) and human epidermal growth factor receptor 2 (Her2). TNBC is associated with a poor prognosis. Previous reports show that aryl hydrocarbon receptor (AhR) partial agonist 2-(4-amino-3-methylphenyl)-5-fluorobenzothiazole (5F 203) selectively inhibits the growth of breast cancer cells including those of the TNBC subtype. We previously demonstrated that 5F 203 induced the expression of putative tumor suppressor gene cytoglobin (CYGB) in breast cancer cells. In the current study, we determined that 5F 203 induces apoptosis and caspase 3 activation in MDA-MB-468 TNBC cells and in T47D ER^+ PR^+ $Her2^-$ breast cancer cells. We also show that caspases and CYGB promote 5F 203-mediated apoptosis in MDA-MB-468 cells. 5F 203 induced lysosomal membrane permeabilization and cathepsin B release in MDA-MB-468 and in T47D cells. Additionally, silencing CYGB attenuated the ability of 5F 203 to induce caspase 3/7 activation, pro-apoptotic gene expression, lysosomal membrane permeabilization and cathepsin B release in MDA-MB-468 cells. Moreover, 5F 203 induced CYGB protein expression, pro-apoptotic protein expression and caspase 3 cleavage in MDA-MB-468 cells and in MDA-MB-468 xenograft tumors grown orthotopically in athymic mice. These data provide a basis for the development of AhR ligands with potential to restore CYGB expression as a novel strategy to treat TNBC.

[*]**Corresponding author**: Eileen Brantley, PhD, 11021 Campus Street, Alumni Hall room 101, Department of Basic Sciences, Loma Linda University Health School of Medicine, Loma Linda, CA 92350, USA. Tel: +1909-558-7703; Fax: +1-909-558-4483, ebrantley@llu.edu.

Conflict of interest

We declare that we have no conflicts of interest.

Keywords

breast cancer; cytoglobin; 5F 203; aryl hydrocarbon receptor; cell death

Introduction

Nearly 40,000 women die each year from breast cancer in the United States and one in eight women will receive a diagnosis in her lifetime. Despite advances in breast cancer treatment, it is still the second leading cause of cancer mortality in women. This death toll is due, in part, to aggressive triple negative breast cancer (TNBC) characterized by tumors that lack expression of the estrogen receptor, progesterone receptor and human epidermal growth factor receptor 2 (HER2). Recently approved poly (ADP-ribose) polymerase inhibitor olaparib primarily benefits TNBC patients with tumors that possess breast cancer type 1 susceptibility protein (BRCA1) mutations [Tutt et al., 2010]. However, many patients with TNBC do not have tumors with BRCA1 mutations and are therefore less responsive to this targeted therapy. Consequently, most patients with TNBC receive chemotherapy, which is associated with severe side effects and recurrence risk.

Emerging data suggest that pharmacological restoration of tumor suppressor genes (TSGs), represents a novel therapeutic approach with potential to benefit TNBC patients [Baylin and Ohm, 2006]. In particular, cytoglobin (CYGB) has been shown to exhibit actions consistent with a tumor suppressor in breast cancer [Shivapurkar et al., 2008]. CYGB expression is absent in most breast tumor tissues but present in adjacent tissues and non-malignant breast epithelial cells [Gorr et al., 2011; Shivapurkar et al., 2008]. The absence of CYGB expression in tumor tissue appears to be primarily due to epigenetic silencing via promoter hypermethylation [Gorr et al., 2011].

We previously discovered that CYGB gene expression is restored when cells are treated with the aryl hydrocarbon receptor (AhR) partial agonist 2-(4-amino-3-methylphenyl)-5-fluorobenzothiazole (5F 203) [McLean et al., 2015]. 5F 203 displays selective and potent anticancer activity *in vitro*, and its prodrug lysylamide derivative (Phortress) is readily bioconverted into 5F 203 to confer anticancer actions *in vivo* [Behrsing et al., 2013; Leong et al., 2003; Leong et al., 2004]. 5F 203 activates AhR signaling to induce DNA damage, cell cycle arrest, and promote apoptotic body formation in MDA-MB-468 cells [Bradshaw et al., 2002; McLean et al., 2015; Trapani et al., 2003]. Other AhR ligands, such as selective aryl hydrocarbon receptor modulators (SAhRMs) show promising anticancer actions in TNBC cells [Jin et al., 2014; O'Donnell et al., 2014; Romagnolo et al., 2015]. Additional studies are needed to fully elucidate the AhR-independent mechanisms of anticancer actions for such ligands.

TSGs confer their actions by regulating cell cycle arrest and apoptosis [Thangavel et al., 2011; Zhou et al., 2010]. However, a comprehensive understanding of CYGB's role in TNBC is lacking. We hypothesize that AhR ligands such as 5F 203 induce CYGB as part of their mechanism of cell death and anticancer action. Our data suggest CYGB promotes the ability of 5F 203 to induce TNBC cell death *in vitro and in vivo*.

Materials & Methods

Cell Culture and Reagents.

MDA-MB-468 (ATCC cat# HTB-138, RRID: CVCL_0419) and T47D (ATCC cat# HTB-133, RRID:CVCL_0553) human breast cancer cells were obtained from the American Type Culture Collection (ATCC) and the Frederick National laboratory for Cancer Research Division of Cancer Treatment and Diagnosis Tumor Repository. The cells were cultured as previously described [McLean et al., 2015]. 2-(4-Amino-3-methylphenyl)-5-fluorobenzothiazole (5F 203, NSC 703786) was obtained from the Frederick National Laboratory for Cancer Research as part of the NCI/DTP Open Chemical Repository (http://dtp.cancer.gov, Frederick, MD). Stock solutions of 5F 203 (10 mM), Staurosporine (1 mM), z-VAD-fmk (100 mM, pan caspase inhibitor) and CH223191 (10 mM, AhR antagonist) were dissolved in dimethyl sulfoxide (DMSO) and stored at −20 °C until use. Phortress, a prodrug lysylamide derivative of 5F 203, was resynthesized in accordance to a previously described method [Hutchinson et al., 2002]. 5F 203 is water insoluble, which limits its usefulness in animal studies. In contrast, Phortress is a prodrug that is water soluble to enable *in vivo* administration. Phortress is readily cleaved by esterases in the body to liberate 5F 203. Antibodies for CYGB (Abnova Corporation Cat# H00114757-A01, RRID:AB_461584), BAK-1 (Cell Signaling Technology Cat# 3814S, RRID:AB_2290287), GADD45a (Cell Signaling Technology Cat# 4632S, RRID:AB_10544538), caspase 3 (Cell Signaling Technology Cat# 9662P, RRID:AB_10839261) and LTA (Abnova Corporation Cat# PAB8441, RRID:AB_1676074) were used. CH223191 and antibodies for β-actin were obtained from Sigma-Aldrich (St. Louis, MO).

Plasmid Transfection.

The CYGB cDNA clones were purchased from OriGene Technologies, Inc (Rockville, MD). MDA-MB-468 cells were transfected with CYGB cDNA using the Oligofectamine reagent in accordance with the manufacturer's instruction. Empty vector cDNA served as a negative control. Stable clones were isolated after cells were transfected for 36 h and subjected to G418 (100ug/mL) media selection.

Lentiviral Transduction.

Lentiviral particles containing short hairpin RNAs (shRNAs) against CYGB or green fluorescent protein (GFP), which served as negative control (Sigma Aldrich), were used to create shCYGB MDA-MB-468 cells and shGFP MDA-MB-468 respectively as described previously [Davidson and Harper, 2005]. The shCYGB sequence corresponded with 5'-CCGG-CCACAGTTGCTTTGAGCACAT-CTCGAG-ATGTGCTCAAAGCAACTGTGG-TTTTTG-3' (Sigma Aldrich). Cells were transduced with MOI of 5 with 8ug/mL of Hexadimethrine bromide (Sigma Aldrich). Stable clones were isolated once cells were subjected to puromycin (5 ug/mL) media selection.

Apoptosis determination.

The Annexin V/Propidium Iodide assay was used to detect apoptosis as previously described [McLean et al., 2008]. Briefly, T47D and MDA-MB-468 cells were treated with 5F 203 (1–

1000 nM respectively) for 24 h. Transduced (shGFP vs shCYGB) and transfected (empty vector vs. CYGB) MDA-MB-468 cells were treated with medium containing 5F 203 or 0.1% DMSO for 24 h. In some studies, MDA-MB-468 cells were pretreated for 1 h with z-VAD-fmk (zVAD, 100 μM) or CH223191 (100nM) before treatment with 5F 203 for 12 h. Data were acquired using a MACSQuant® Analyzer 10 (Miltenyi Biotec Inc., Auburn, CA) and analyzed using FlowJo (v9.7.5, Tree Star, Inc., Ashland, OR).

Caspase activity assay.

T47D and MDA-MB-468 cells were treated with 0.1% DMSO or 5F 203 (1 μM, 12 h) before employing the caspase 3 activity as described [McLean et al., 2008]. Alternatively, MDA-MB-468 cells were incubated at 37 °C for 1 h with fluorescent-labeled caspase inhibitor FAM-VAD-FMK probes (FLICA reagent) for caspases-3 and 7 according to the manufacturer's instructions (Immunochemistry Technologies, Bloomington, MN, USA). Data were acquired using a MACSQuant® Analyzer 10 and analyzed as stated above with the method to determine apoptosis.

Evaluation of Lysosomal Membrane Permeabilization.

The Acridine Orange (AO, ImmunoChemistry Technologies, Bloomington, MN) assay was used to determine lysosomal membrane permeabilization (LMP) as described previously [Almaguel et al., 2010]. Briefly, MDA-MB-468 cells, (including shGFP vs. shCYGB) and T47D cells were seeded at 4×10^5 cells/well in 6-well culture plates and incubated overnight before treatment with 0.1% DMSO or 5F 203 for 24 h. The cells were washed with cold PBS and exposed to medium containing 5 μM AO and counterstained with 5 μM Hoechst 33342. The cells were incubated for 30 min at 37°C. Cell images were captured with an Olympus IX-71 microscope with fluorescence imaging or a fluorescence microscope equipped with an EVOS cell imaging system (Invitrogen, USA).

Cathepsin B Release Determination.

The fluorogenic substrate-based assay, Magic Red (Immunochemistry Technologies, Bloomington, MN), was used to detect Capthesin B release as described previously [Almaguel et al., 2010]. Briefly, T47D and MDA-MB-468 cells (including shGFP vs. shCYBG) were treated with 0.1% DMSO or 5F 203 for 24 h. Cells were exposed to cathepsin B substrate MR-$(RR)_2$ for 45 min, rinsed twice with cold PBS, and counterstained with Hoechst 33342 to detect nuclear morphology before images were captured as described above to determine lysosomal membrane permeabilization.

Immunoblotting.

MDA-MB-468 cells were seeded at $1–3 \times 10^6$ per plate (100 mm) 24 h before cells were treated with medium containing 1 μM 5F 203 or 0.1% DMSO for 72h. Following treatment, cells were harvested and Western blotting performed as described [McLean et al., 2015]. Briefly, proteins were resolved on 4–12% SDS-polyacrylamide gels and transferred to nitrocellulose membranes. The membranes were blocked before overnight incubation at 4 °C in 5% BSA-based buffer with mouse primary antibodies against CYGB (1:200 dilution), LTA (1:1000), and rabbit primary antibodies against BAK-1 (1:1000), GADD45A (1:1000)

and Caspase 3 (1:1000). Membranes were incubated with the appropriate HRP-conjugated secondary antibodies (Cell Signaling Technology, Danvers MA or Santa Cruz Biotechnology, Santa Cruz, CA) for 1 h at the appropriate dilution before imaging.

Apoptosis RT^2 Profiler PCR Array.

MDA-MB-468 cells were treated with 100 nM 5F 203 for 24 h before RNA was extracted. Extracts were analyzed using the apoptosis RT^2 Profiler ® PCR Array (PAHS-012Z, Qiagen, USA) according to the manufacture's instructions (SA Biosciences, Frederick, MD, USA) as previously described [McLean et al., 2015].

Real-Time Quantitative RT-PCR (qPCR) Analysis.

RNA was extracted from breast cancer cells following specified treatments and cDNA synthesis performed according to the manufacturer's instructions and in accordance to a method previously described [McLean et al., 2015]. The primers for the GAPDH, CYGB, LTA, BAK1, and GADD45A genes were obtained from SA Biosciences (Frederick, MD). Relative fold changes in gene expression were calculated using the $2^{-\Delta\Delta C_T}$ method.

Colony Formation and Wound Healing Assays.

MDA-MB-468 cells transfected to overexpress CYGB or empty vector were plated at a density of 200 cells per well in a 6 well plate and allowed to grow for 2 weeks before the cells were stained with Crystal Violet and colonies counted manually. For the Wound healing assay, MDA-MB-468 cells (including shGFP vs shCYGB) were plated in 24-well plates at a density of 200,000 cells/ well, and allowed to recover overnight, before a wound was made using a 10 μl pipet tip. The cells were then treated with 0.1% DMSO or 100 nM 5F 203 for 24 h. Images were captured on an Olympus IX-71 microscope and quantified using SPOT software (Diagnostic Instruments, Inc.).

In vivo study.

Five to six week old female athymic nude mice (CRL: NU(NCr)-Foxn1nu, Charles River, strain 490) were obtained from Charles Rivers Laboratory (San Diego, CA) and housed under pathogen-free conditions. Animals were fed an autoclaved laboratory rodent diet and allowed to acclimatize for two weeks before any experiments were initiated. The Institutional Animal Care and Use Committee (IACUC) at Loma Linda University Health approved the animal studies which were carried out in Loma Linda's AALAC-accredited Animal Care Facility in specially assigned rooms for the immunodeficient athymic mice (protocol #8130059). All procedures were performed in compliance with principles and procedures outlined in the National Institutes of Health Guide for the Care and Use of Animals under Assurance number A3873–1. MDA-MB-468 cells (5×10^6) were placed in a suspension 50/50 ratio (100 μL: 100 μL) of Corning® Matrigel® Matrix (Corning, NY) and injected orthotopically into the right mammary fat pad of mice under isoflurane anesthesia. Once tumors in mice were palpable (~50 mm^3), they were measured twice a week with a digital caliper in two planes (length and width) for the remaining weeks of the study. Tumor volume was calculated using the formula: (length × width^2)/2. For animal dosing, Phortress was prepared in phosphate buffered saline (PBS) solution. Each experiment contained a

control group ($n = 11$) treated with PBS in parallel with a Phortress-treated group (n = 11). Once tumors reached an average size of 150 mm^3, the animals received intraperitoneal (i.p.) injections of either the vehicle (saline) or Phortress (15mg/kg) administered using a Q2D X 3 schedule followed by a 10 d rest period for a total of 3 cycles. To alleviate symptoms of toxicity, animals received Phortress (7.5mg/kg) for the last two cycles. The animals were sacrificed using CO_2 inhalation and tumors excised 24 h after the final dose.

Tumor protein extraction and immunoblotting.

For protein analysis, MDA-MB-468 xenograft tumors were immediately snap frozen after excision and stored in liquid nitrogen. Frozen tumors were lysed using a spring scissors in Lysis Buffer and protein concentration was determined using the D_C protein assay kit according to the manufacturer's instructions (Bio-Rad, Hercules, CA). Proteins were resolved and imaged as described above for MDA-MB-468 cells.

Statistical Analysis.

Data are reported as mean ± SEM. Statistical significance was assessed using either the one-way ANOVA with Tukey's test or the Tukey-Kramer multiple comparison test when using three or more groups. To compare two groups, an unpaired Student's t test with Welch's correction was used. Statistical analysis was performed using GraphPad Instat 3.0. Differences were considered significant at $p < 0.05$.

Results

CYGB and caspases promote 5F 203-mediated apoptosis in TNBC cells.

AhR represents a potential drug target for TNBC [Gilbert et al., 2018; Safe et al., 2017]. We previously demonstrated that 5F 203 induces CYGB mRNA expression and promotes apoptotic body formation in MDA-MB-468 cells [McLean et al., 2015]. CYGB has been found to stabilize p53, a major player in a broad range of cellular processes such as cell cycle arrest and cell death [Aubrey et al., 2017; John et al., 2014]. We show that 5F 203 promotes dose-dependent increases in apoptosis in T47D and MDA-MB-468 cells, as evidenced by an increase in cells that stain positive for Annexin V (Figure 1A). 5F 203 (1 μM, 12 and 24h) also promoted caspase 3 activation in these cells (Figure 1B,D). Next, we created cells to stably overexpress or knockdown CYGB to more clearly delineate the role of CYGB in 5F 203-mediated apoptosis and caspase activation. We found that knockdown of CYGB substantially impaired the ability of 5F 203 to induce CYGB expression. (Figure 1C). Our data reveal that CYGB knockdown diminishes 5F 203-mediated apoptosis and caspase 3/7 activation (Figure 1E). Enforced expression of CYGB in MDA-MB-468 cells promoted both apoptosis and caspase 3/7 activation (Figure 1F). Although 5F 203 was unable to further increase apoptosis in cells enforced to overexpress CYGB, it significantly enhanced caspase 3/7 activation (Figure 1G).

We previously demonstrated that AhR antagonist α-naphthoflavone decreased the ability of 5F 203 to increase apoptotic body formation and induce CYGB expression in MDA-MB-468 cells [McLean et al., 2015]. In the current study, we used the potent and specific AhR antagonist CH223191 to confirm that AhR mediates the ability of 5F 203 to induce

apoptosis in MDA-MB-468 cells. Our data show that CH223191 significantly diminished 5F 203-mediated apoptosis in MDA-MB-468 cells, to suggest that 5F 203 relies at least partially on its ability to activate AhR signaling to confer cell death (Figure 2A).

To further identify the role of CYGB in 5F 203-mediated apoptosis induction, we analyzed the expression of three pro-apoptotic genes following treatment in shCYGB and shGFP MDA-MB-468 cells. These genes include: Bcl-2 homologous antagonist killer (BAK-1), which promotes apoptosis and counteracts protection from apoptosis provided by Bcl-2 [Chittenden et al., 1995]; Growth arrest and DNA-damage-inducible protein alpha (GADD45a), which contributes to p53 activation via p38 [Salvador et al., 2013]; and Lymphotoxin-alpha (LTA), which induces tumor necrosis factor receptor 1 (TNFR1)-dependent apoptosis and necroptosis [Etemadi et al., 2013]. These genes were identified in an apoptosis regulatory gene PCR array as induced more than 3-fold following 5F 203 treatment (Table 1) and their expression verified using quantitative real-time PCR (Figure 2B). We found an attenuation in 5F 203-induced expression of pro-apoptotic BAK-1 and LTA in shCYGB cells relative to shGFP cells (Figure 2C). Taken together, our data show that AhR signaling activation and CYGB promote 5F 203-induced apoptosis, caspase 3/7 activation and BAK-1 and LTA mRNA expression in MDA-MB-468 cells.

Next, we sought to determine whether 5F 203-mediated cell death was caspase-dependent. We treated MDA-MB-468 cells with 0.1% DMSO (negative control), Staurosporine (STS, positive control) and 5F 203 for 12 h in the presence or absence of z-VAD. Our data show that z-VAD pretreatment caused a statistically significant decrease in the ability of 5F 203 to induce apoptosis in these cells. These data reveal that caspases promote 5F 203-mediated cell death (Figure 2D). Our data show that the inhibition was not complete, suggesting that 5F 203 also induces caspase-independent cell death.

CYGB promotes lysosomal membrane permeabilization and cathepsin B release in breast cancer cells treated with 5F 203.

Organelles such as lysosomes are involved in mediating cell death. Lysosomal membrane permeabilization (LMP) promotes the selective liberation of cathepsins such as cathepsin B into the cytoplasm triggering both caspase-dependent and caspase-independent cell death pathways [Serrano-Puebla and Boya, 2016]. Additionally, LMP has been found to depend, at least in part, on AhR signaling activation [Caruso et al., 2006; Johansson et al., 2010]. We used acridine orange and magic red assays to measure LMP and cathepsin B release respectively. We found that 5F 203 treatment caused LMP, as evidenced by a reduction in intact, punctate red lysosomes in MDA-MB-468 cells and to a lesser extent in T47D cells (Figure 3A). In addition, 5F 203 promoted cathepsin B release, characterized by diffuse red fluorescent dye staining (Figure 3B). Our data also show that 5F 203-mediated LMP and cathepsin B release were attenuated in shCYGB MDA-MB-468 cells relative to shGFP MDA-MB-468 cells (Figure 3C,D). This suggests CYGB promotes 5F 203-mediated LMP and cathepsin B release in MDA-MB-468 cells.

5F 203 promotes anticancer activity, induces CYGB expression, and alters pro-apoptotic protein expression *in vitro and in vivo*.

To determine whether CYGB decreases proliferation of MDA-MB-468 cells, empty vector and CYGB over-expressing MDA-MB-468 cells were subjected to a colony forming assay. We found that CYGB overexpressing cells resulted in substantially fewer colonies as compared to empty vector and non-transfected cells (Figure 4A). This corroborates findings in a previous study involving cancer cells enforced to express CYGB [Shivapurkar et al., 2008]. We performed a wound healing assay to determine whether CYGB impacts the ability of 5F 203 to decrease cell migration. Our data showed that silencing CYGB attenuated 5F 203-mediated inhibition of wound healing (Figure 4B) to suggest CYGB contributes to the ability of 5F 203 to suppress cancer cell migration, which precedes cancer cell invasion and metastases.

We previously found that 5F 203 induced CYGB gene expression in a panel of cells [McLean et al., 2015] and in the current study we found 5F 203 induced CYGB protein expression (Figure 4C). In addition, 5F 203 induced the expression of pro-apoptotic proteins BAK-1, GADD45a and LTA, in agreement with the induced gene expression observed in Figure 2B. Caspase 3 cleavage was also detected in MDA-MB-468 cells exposed to 5F 203 (Figure 4 C,D). CYGB silencing diminished the ability of 5F 203 to induce the expression of GADD45a and LTA as well as caspase cleavage but not BAK-1 to suggest 5F 203-mediated induction of BAK-1 protein expression does not rely on CYGB.

To investigate the impact of 5F 203 on *in vivo* cell growth, we treated athymic mice bearing MDA-MB-468 xenografts with Phortress, the prodrug formulation of 5F 203, synthesized as previously described to improve water solubility [Leong et al., 2003]. Phortress caused a 40% reduction (DMSO= 348.7±79.7, Phortress= 202.7±24.9) in tumor volume and a significant reduction in tumor weight (Figure 5 A,B). To determine whether inhibition of tumor growth was associated with induced CYGB expression, tumors were lysed and subjected to immunoblotting to measure CYGB protein expression. Phortress increased CYGB protein expression in tumors (Figure 5 C,D). Additionally, Phortress increased the expression of BAK-1 and GADD45A as well as promoted caspase 3 cleavage in MDA-MB-468 xenograft tumors (Figure 5 C,D).

Discussion

It is crucial to develop agents with the capacity to effectively treat TNBC since clinical outcomes for patients with this malignancy are dismal. Indeed, AhR has been proposed as a potential target for TNBC and the data from our studies suggest CYGB represents another plausible target. We found that AhR ligand 5F 203 induced the expression of CYGB *in vitro* and to a lesser extent *in vivo*. We also showed that CYGB promoted 5F 203-mediated TNBC cell death, while promoting lysosomal instability, cathepsin B release and suppressing TNBC cell migration.

We previously demonstrated that 5F 203 induces AhR-dependent CYGB expression [McLean et al., 2015]. 5F 203 induced CYGB in the highly AhR-responsive MDA-MB-468 cells but not the far less AhR-responsive MDA-MB-231 cells [McLean et al., 2015]. Others

have demonstrated the potential for small molecules to activate AhR signaling as a strategy to treat breast cancer [Gilbert et al., 2018; Jang et al., 2017; Safe et al., 2017]. More specifically, SAhRMs have been suggested as potential agents to treat TNBC since TNBC tumors exhibit higher AhR expression compared to luminal (ER+) and HER-2+ breast tumors [Romagnolo et al., 2015]. We and others have shown that certain AhR ligands induce apoptosis in TNBC cells [Brinkman et al., 2014; Jin et al., 2012; McLean et al., 2008; McLean et al., 2015; Narasimhan et al., 2018; Powell et al., 2013; Stark et al., 2013; Wang et al., 1997; Wang et al., 2017; Zhang et al., 2009].

Apoptosis is a complex and highly regulated process of cell death that is essential for tissue homeostasis [Hassan et al., 2014]. Many cancers, including breast cancer, support their survival by deregulating apoptosis induced by therapies, which makes it paramount to understand the mechanism(s) used to evade cell death [Deshmukh et al., 2017; Hanahan and Weinberg, 2011]. In this study, we observed that silencing CYGB reduced 5F 203-mediated apoptosis, caspase 3/7 activation, lysosomal membrane permeabilization, and cathepsin B release. Therefore, 5F 203's ability to "reactivate" CYGB appears to aid in its ability to promote TNBC cell death.

We found that 5F 203 suppressed TNBC cell migration to suggest that it has the capacity to arrest the progression of TNBC. 5F 203 was less able to suppress TNBC migration in shCYGB cells as compared to shGFP cells (Figure 4B). In contrast we found that 5F 203 mediated suppression of TNBC cell proliferation persisted despite shCYBG knockdown (data not shown). Our data also indicated that while Phortress induced CYGB expression *in vivo*, this agent induced the expression of pro-apoptotic proteins BAK1 and GADD45a to a much greater extent (Figure 5C,D). This suggests that CYGB plays a pivotal role in TNBC migration and TNBC cell death, but not in 5F 203-mediated antiproliferative activity *in vitro* and *in vivo*.

The silencing of CYGB by methylation has been reported in a variety of malignancies [Shivapurkar et al., 2008]. Furthermore, higher levels of CYGB methylation correlate with more aggressive breast cancers, including TNBC [Zhang et al., 2015]. Additionally CYGB stabilizes p53, a key cellular DNA damage signal factor [John et al., 2014]. CYGB reduces p53 ubiquitination, which increases its half-life three-fold. The silencing of CYGB appears to enable cancer cells to evade cell death and progress through the cell cycle.

In conclusion, our study suggests CYGB aids in promoting cell death and migration once AhR signaling activation occurs. CYGB reactivation represents a potential therapeutic approach for TNBC. Our study provides a rationale for future investigations examining AhR ligand-mediated upregulation of CYGB to treat not only TNBC but other aggressive malignancies.

Acknowledgements

The authors thank Dr. Melinda Hollingshead in providing helpful suggestions for the animal studies and Dr. Christina Cajigas-Du Ross for assistance with immunoblotting. The authors also thank Drs. Maheswari Senthil and Gayathri Nagaraj for helpful discussions. This research was supported in part from Grants to Promote Collaborative and Translational Research (GCAT), Grants for Research and School Partnerships (GRASP), the LLU School of Medicine Basic Science Dean's Stipend Support, LLU School of Medicine Center for Health Disparities and

Molecular Medicine, the LLU School of Pharmacy Department of Pharmaceutical and Administrative Sciences as well as the following National Institutes of Health grants: National Institute of General Medical Sciences (award numbers 5R25GM082808 and R25GM060507) and National Institute on Minority Health and Health Disparities (award number P20MD006988).

References

Almaguel FG, Liu JW, Pacheco FJ, De Leon D, Casiano CA, De Leon M. 2010 Lipotoxicity-mediated cell dysfunction and death involve lysosomal membrane permeabilization and cathepsin L activity. Brain Res 1318:133–43. 10.1016/j.brainres.2009.12.038. [PubMed: 20043885]

Aubrey BJ, Kelly GL, Janic A, Herold MJ, Strasser A. 2017 How does p53 induce apoptosis and how does this relate to p53-mediated tumour suppression? Cell Death And Differentiation 25:104 10.1038/cdd.2017.169. [PubMed: 29149101]

Baylin SB, Ohm JE. 2006 Epigenetic gene silencing in cancer - a mechanism for early oncogenic pathway addiction? Nat Rev Cancer 6:107–16. [PubMed: 16491070]

Behrsing HP, Furniss MJ, Davis M, Tomaszewski JE, Parchment RE. 2013 In vitro exposure of precision-cut lung slices to 2-(4-amino-3-methylphenyl)-5-fluorobenzothiazole lysylamide dihydrochloride (NSC 710305, Phortress) increases inflammatory cytokine content and tissue damage. Toxicol Sci 131:470–9. 10.1093/toxsci/kfs319. [PubMed: 23143926]

Bradshaw TD, Bibby MC, Double JA, Fichtner I, Cooper PA, Alley MC, Donohue S, Stinson SF, Tomaszewjski JE, Sausville EA, Stevens MF. 2002 Preclinical evaluation of amino acid prodrugs of novel antitumor 2-(4-amino-3-methylphenyl)benzothiazoles. Mol Cancer Ther 1:239–46. [PubMed: 12467219]

Brinkman AM, Wu J, Ersland K, Xu W. 2014 Estrogen receptor α and aryl hydrocarbon receptor independent growth inhibitory effects of aminoflavone in breast cancer cells. BMC Cancer 14:344–344. 10.1186/1471-2407-14-344. [PubMed: 24885022]

Caruso JA, Mathieu PA, Joiakim A, Zhang H, Reiners JJ. 2006 Aryl Hydrocarbon Receptor Modulation of Tumor Necrosis Factor-α-induced Apoptosis and Lysosomal Disruption in a Hepatoma Model That Is Caspase-8-independent. Journal of Biological Chemistry 281:10954–10967. [PubMed: 16446372]

Chittenden T, Harrington EA, O'Connor R, Remington C, Lutz RJ, Evan GI, Guild BC. 1995 Induction of apoptosis by the Bcl-2 homologue Bak. Nature 374:733. [PubMed: 7715730]

Davidson BL, Harper SQ. 2005 Viral delivery of recombinant short hairpin RNAs. Methods Enzymol 392:145–73. [PubMed: 15644180]

Deshmukh SK, Srivastava SK, Zubair H, Bhardwaj A, Tyagi N, Al-Ghadhban A, Singh AP, Dyess DL, Carter JE, Singh S. 2017 Resistin potentiates chemoresistance and stemness of breast cancer cells: Implications for racially disparate therapeutic outcomes. Cancer Lett 396:21–29. 10.1016/j.canlet.2017.03.010. [PubMed: 28302531]

Etemadi N, Holien JK, Chau D, Dewson G, Murphy JM, Alexander WS, Parker MW, Silke J, Nachbur U. 2013 Lymphotoxin α induces apoptosis, necroptosis and inflammatory signals with the same potency as tumour necrosis factor. FEBS Journal 280:5283–5297. 10.1111/febs.12419. [PubMed: 23815148]

Gilbert J, De Iuliis GN, Tarleton M, McCluskey A, Sakoff JA. 2018 (Z)-2-(3,4-Dichlorophenyl)-3-(1H-Pyrrol-2-yl)Acrylonitrile Exhibits Selective Antitumor Activity in Breast Cancer Cell Lines via the Aryl Hydrocarbon Receptor Pathway. Molecular Pharmacology 93:168–177. 10.1124/mol.117.109827. [PubMed: 29269419]

Gorr TA, Wichmann D, Pilarsky C, Theurillat JP, Fabrizius A, Laufs T, Bauer T, Koslowski M, Horn S, Burmester T, Hankeln T, Kristiansen G. 2011 Old proteins - new locations: myoglobin, haemoglobin, neuroglobin and cytoglobin in solid tumours and cancer cells. Acta Physiol (Oxf) 202:563–81. 10.1111/j.1748-1716.2010.02205.x. [PubMed: 20958924]

Hanahan D, Weinberg RA. 2011 Hallmarks of cancer: the next generation. Cell 144:646–74. 10.1016/j.cell.2011.02.013. [PubMed: 21376230]

Hassan M, Watari H, AbuAlmaaty A, Ohba Y, Sakuragi N. 2014 Apoptosis and Molecular Targeting Therapy in Cancer. BioMed Research International 2014:150845 10.1155/2014/150845. [PubMed: 25013758]

Hutchinson I, Jennings SA, Vishnuvajjala BR, Westwell AD, Stevens MF. 2002 Antitumor benzothiazoles. 16. Synthesis and pharmaceutical properties of antitumor 2-(4-aminophenyl)benzothiazole amino acid prodrugs. J Med Chem 45:744–7. [PubMed: 11806726]

Jang HS, Pearce M, O'Donnell EF, Nguyen BD, Truong L, Mueller MJ, Bisson WH, Kerkvliet NI, Tanguay RL, Kolluri SK. 2017 Identification of a Raloxifene Analog That Promotes AhR-Mediated Apoptosis in Cancer Cells. Biology (Basel) 6 10.3390/biology6040041.

Jin UH, Lee SO, Pfent C, Safe S. 2014 The aryl hydrocarbon receptor ligand omeprazole inhibits breast cancer cell invasion and metastasis. BMC Cancer 14:498 10.1186/1471-2407-14-498. [PubMed: 25011475]

Jin UH, Lee SO, Safe S. 2012 Aryl hydrocarbon receptor (AHR)-active pharmaceuticals are selective AHR modulators in MDA-MB-468 and BT474 breast cancer cells. J Pharmacol Exp Ther 343:333–41. 10.1124/jpet.112.195339. [PubMed: 22879383]

Johansson A-C, Appelqvist H, Nilsson C, Kågedal K, Roberg K, Öllinger K. 2010 Regulation of apoptosis-associated lysosomal membrane permeabilization. Apoptosis 15:527–540. 10.1007/s10495-009-0452-5. [PubMed: 20077016]

John R, Chand V, Chakraborty S, Jaiswal N, Nag A. 2014 DNA damage induced activation of Cygb stabilizes p53 and mediates G1 arrest. DNA Repair 24:107–112. 10.1016/j.dnarep.2014.09.003. [PubMed: 25269893]

Leong CO, Gaskell M, Martin EA, Heydon RT, Farmer PB, Bibby MC, Cooper PA, Double JA, Bradshaw TD, Stevens MF. 2003 Antitumour 2-(4-aminophenyl)benzothiazoles generate DNA adducts in sensitive tumour cells in vitro and in vivo. Br J Cancer 88:470–7. [PubMed: 12569393]

Leong CO, Suggitt M, Swaine DJ, Bibby MC, Stevens MF, Bradshaw TD. 2004 In vitro, in vivo, and in silico analyses of the antitumor activity of 2-(4-amino-3-methylphenyl)-5-fluorobenzothiazoles. Mol Cancer Ther 3:1565–75. [PubMed: 15634650]

McLean L, Soto U, Agama K, Francis J, Jimenez R, Pommier Y, Sowers L, Brantley E. 2008 Aminoflavone induces oxidative DNA damage and reactive oxidative species-mediated apoptosis in breast cancer cells. Int J Cancer 122:1665–74. [PubMed: 18059023]

McLean LS, Watkins CN, Campbell P, Zylstra D, Rowland L, Amis LH, Scott L, Babb CE, Livingston WJ, Darwanto A, Davis WL, Jr., Senthil M, Sowers LC, Brantley E. 2015 Aryl Hydrocarbon Receptor Ligand 5F 203 Induces Oxidative Stress That Triggers DNA Damage in Human Breast Cancer Cells. Chem Res Toxicol 28:855–71. 10.1021/tx500485v. [PubMed: 25781201]

Narasimhan S, Stanford Zulick E, Novikov O, Parks AJ, Schlezinger JJ, Wang Z, Laroche F, Feng H, Mulas F, Monti S, Sherr DH. 2018 Towards Resolving the Pro- and Anti-Tumor Effects of the Aryl Hydrocarbon Receptor. International Journal of Molecular Sciences 19:1388 10.3390/ijms19051388.

O'Donnell EF, Koch DC, Bisson WH, Jang HS, Kolluri SK. 2014 The aryl hydrocarbon receptor mediates raloxifene-induced apoptosis in estrogen receptor-negative hepatoma and breast cancer cells. Cell Death Dis 5:e1038 10.1038/cddis.2013.549. [PubMed: 24481452]

Powell JB, Goode GD, Eltom SE. 2013 The Aryl Hydrocarbon Receptor: A Target for Breast Cancer Therapy. Journal of cancer therapy 4:1177–1186. [PubMed: 25068070]

Quintana F, Basso A, Iglesias A, Korn T, Farez M, Bettelli E, Caccamo M, Oukka M, Weiner H. 2008 Control of T(reg) and T(H)17 cell differentiation by the aryl hydrocarbon receptor. Nature 453:65–71. 10.1038/nature06880. [PubMed: 18362915]

Romagnolo DF, Papoutsis AJ, Laukaitis C, Selmin OI. 2015 Constitutive expression of AhR and BRCA-1 promoter CpG hypermethylation as biomarkers of ERα-negative breast tumorigenesis. BMC Cancer 15:1026 10.1186/s12885-015-2044-9. [PubMed: 26715507]

Safe S, Cheng Y, Jin U-H. 2017 The Aryl Hydrocarbon Receptor (AhR) as a Drug Target for Cancer Chemotherapy. Current opinion in toxicology 2:24–29. 10.1016/j.cotox.2017.01.012. [PubMed: 28459113]

Salvador JM, Brown-Clay JD, Fornace AJ. 2013 Gadd45 in Stress Signaling, Cell Cycle Control, and Apoptosis. In Liebermann DA, Hoffman B, editor^editors. Gadd45 Stress Sensor Genes. New York, NY: Springer New York, p 1–19.

Serrano-Puebla A, Boya P. 2016 Lysosomal membrane permeabilization in cell death: new evidence and implications for health and disease. Annals of the New York Academy of Sciences 1371:30–44. 10.1111/nyas.12966. [PubMed: 26599521]

Shivapurkar N, Stastny V, Okumura N, Girard L, Xie Y, Prinsen C, Thunnissen FB, Wistuba II, Czerniak B, Frenkel E, Roth JA, Liloglou T, Xinarianos G, Field JK, Minna JD, Gazdar AF. 2008 Cytoglobin, the newest member of the globin family, functions as a tumor suppressor gene. Cancer Res 68:7448–56. 10.1158/0008-5472.CAN-08-0565. [PubMed: 18794132]

Stark K, Burger A, Wu J, Shelton P, Polin L, Li J. 2013 Reactivation of estrogen receptor alpha by vorinostat sensitizes mesenchymal-like triple-negative breast cancer to aminoflavone, a ligand of the aryl hydrocarbon receptor. PLoS One 8:e74525 10.1371/journal.pone.0074525. [PubMed: 24058584]

Thangavel C, Dean JL, Ertel A, Knudsen KE, Aldaz CM, Witkiewicz AK, Clarke R, Knudsen ES. 2011 Therapeutically activating RB: reestablishing cell cycle control in endocrine therapy-resistant breast cancer. Endocr Relat Cancer 18:333–45. 10.1530/ERC-10-0262. [PubMed: 21367843]

Trapani V, Patel V, Leong CO, Ciolino HP, Yeh GC, Hose C, Trepel JB, Stevens MF, Sausville EA, Loaiza-Perez AI. 2003 DNA damage and cell cycle arrest induced by 2-(4-amino-3-methylphenyl)-5-fluorobenzothiazole (5F 203, NSC 703786) is attenuated in aryl hydrocarbon receptor deficient MCF-7 cells. Br J Cancer 88:599–605. [PubMed: 12592376]

Tutt A, Robson M, Garber JE, Domchek SM, Audeh MW, Weitzel JN, Friedlander M, Arun B, Loman N, Schmutzler RK, Wardley A, Mitchell G, Earl H, Wickens M, Carmichael J. 2010 Oral poly(ADP-ribose) polymerase inhibitor olaparib in patients with BRCA1 or BRCA2 mutations and advanced breast cancer: a proof-of-concept trial. Lancet 376:235–44. 10.1016/S0140-6736(10)60892-6. [PubMed: 20609467]

Wang WL, Porter W, Burghardt R, Safe SH. 1997 Mechanism of inhibition of MDA-MB-468 breast cancer cell growth by 2,3,7,8-tetrachlorodibenzo-p-dioxin. Carcinogenesis 18:925–33. [PubMed: 9163677]

Wang Y, Wang Y, Chen G, Li Y, Xu W, Gong S. 2017 Quantum-Dot-Based Theranostic Micelles Conjugated with an Anti-EGFR Nanobody for Triple-Negative Breast Cancer Therapy. ACS Appl Mater Interfaces 9:30297–30305. 10.1021/acsami.7b05654. [PubMed: 28845963]

Zhang C, Zhao H, Li J, Liu H, Wang F, Wei Y, Su J, Zhang D, Liu T, Zhang Y. 2015 The Identification of Specific Methylation Patterns across Different Cancers. PLOS ONE 10:e0120361 10.1371/journal.pone.0120361. [PubMed: 25774687]

Zhang S, Lei P, Liu X, Li X, Walker K, Kotha L, Rowlands C, Safe S. 2009 The aryl hydrocarbon receptor as a target for estrogen receptor-negative breast cancer chemotherapy. Endocr Relat Cancer 16:835–44. 10.1677/ERC-09-0054. [PubMed: 19447902]

Zhou Z, Thomsen R, Kahns S, Nielsen AL. 2010 The NSD3L histone methyltransferase regulates cell cycle and cell invasion in breast cancer cells. Biochem Biophys Res Commun 398:565–70. 10.1016/j.bbrc.2010.06.119. [PubMed: 20599755]

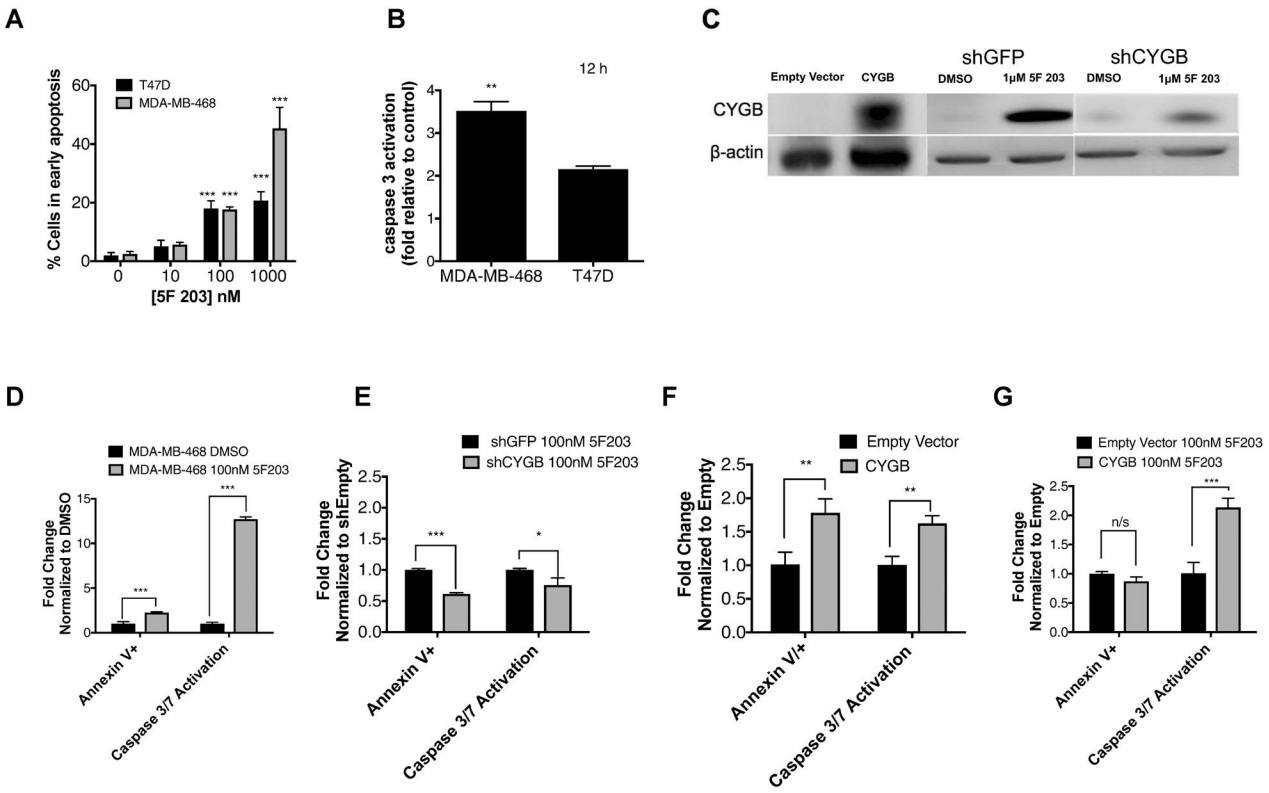

Figure 1. CYGB contributes to 5F 203-mediated caspase activation and apoptosis induction.

(A) Determination of apoptosis via the Annexin V/PI assay in T47D and MDA-MB-468 cells exposed to media containing 0.1% DMSO or 5F 203 (1–1000 nM) for 24 h. (B) Caspase activity evaluation in T47D and MDA-MB-468 cells treated with media containing 0.1% DMSO or 5F 203 (1μM). (C) Immunoblot verification of enforced CYGB expression in MDA-MB-468 cells as well as CYGB expression in shCYGB and shGFP MDA-MB-468 cells following treatment with 5F 203. (D) Apoptosis and caspase activity determination in MDA-MB-468 cells following treatment with 5F 203. (E) Apoptosis and caspase activity determination in shCYGB or shGFP MDA-MB-468 cells following treatment with 0.1% DMSO or 100 nM 5F 203. (F-G) Apoptosis and caspase activity determination in MDA-MB-468 cells stably transfected to overexpress CYGB vs. empty vector without treatment (F) or with 5F 203 treatment (G). Bars, SEM. Statistically significant in comparison to control or where indicated as designated * $P < 0.05$, ** $P < 0.01$ or *** $P < 0.001$.

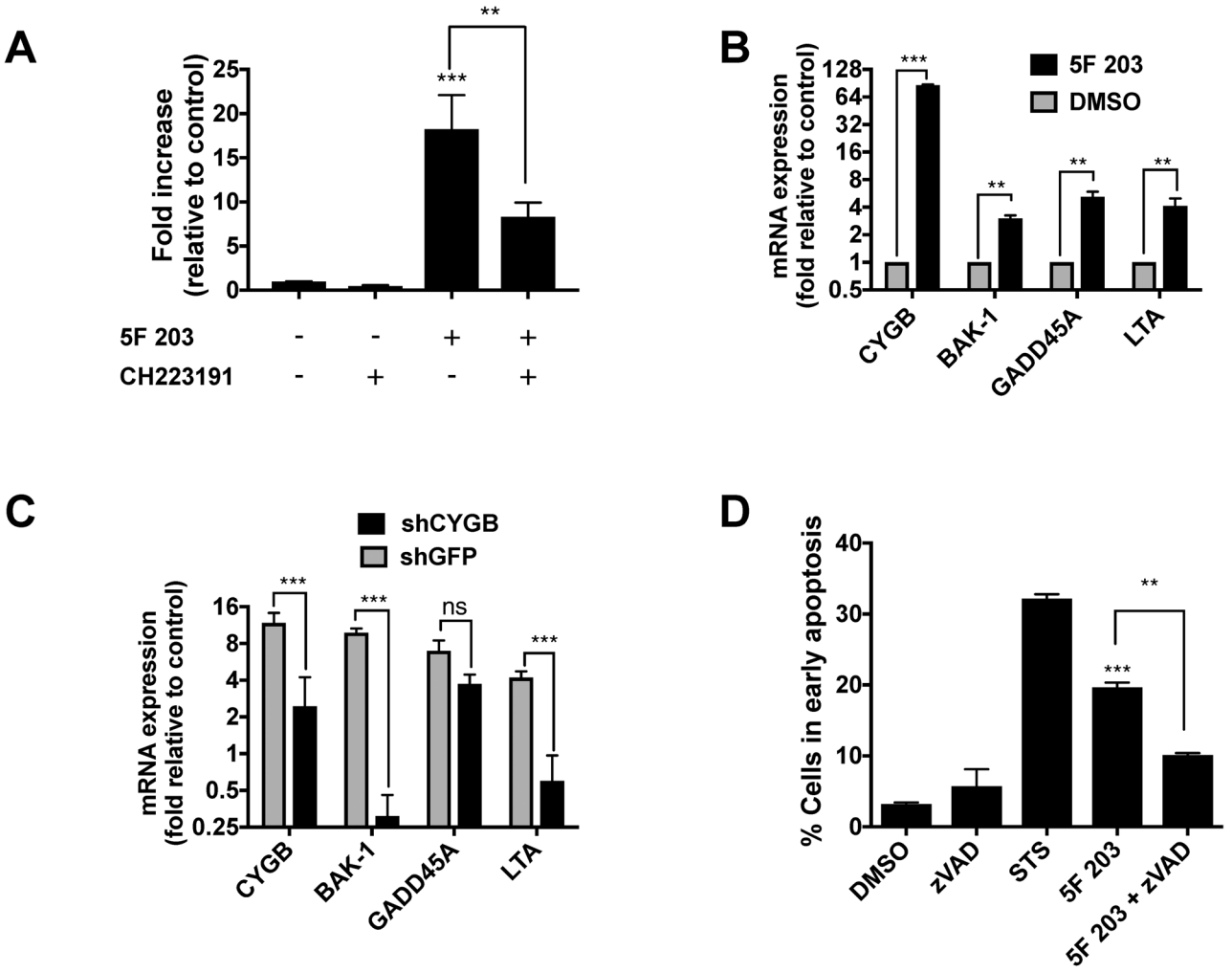

Figure 2. 5F 203 promotes AhR-, CYGB- and caspase-dependent cell death.

(A) Apoptosis evaluation (fold increase in early apoptosis) in cells exposed to 0.1% DMSO (negative control), AhR antagonist CH223191 (100 nM), 5F 203 (1μM) or 5F 203 for 12 h in the presence or absence of 1 h CH223191 pretreatment. (B) CYGB, BAK-1, GADD45A and LTA mRNA expression following treatment with 5F 203 (24h) in MDA-MB-468 cells. (C) CYGB, BAK-1, GADD45A and LTA mRNA expression following 5F 203 (100 nM, 24h) treatment in shCYGB or shGFP cells. (D) Apoptosis evaluation in cells exposed to 0.1% DMSO (negative control), Staurosporine (STS, positive control), or 5F 203 (100 nM, 12 h) in the presence or absence of pretreatment with z-VAD-fmk (ZVAD, pan caspase inhibitor) for 1h. Bars, SEM. Statistically significant in comparison to control (DMSO) or where indicated as designated **P < 0.01 or ***P < 0.001.

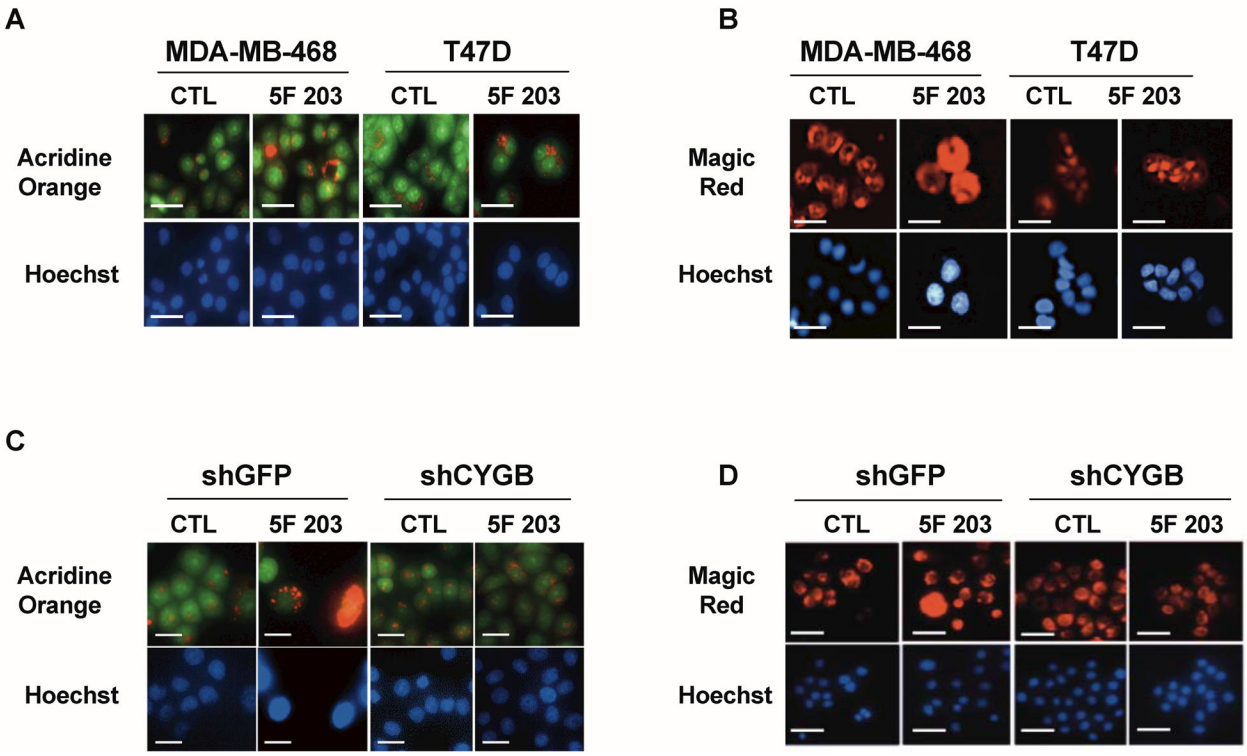

Figure 3. 5F 203 induces CYGB-dependent lysosomal membrane permeabilization and cathepsin B release

(A,B) T47D and MDA-MB-468 cells following treatment with 0.1% DMSO (CTL) or 5F 203 (1μM for T47D cells and 100 nM for MDA-MB-468 cells) for 24 h followed by analysis using Acridine Orange or the Magic Red assays to measure LMP and cathepsin B release respectively. (C,D) shCYGB and shGFP MDA-MB-468 cells evaluated for LMP and cathepsin B release respectively following 5F 203 treatment. Scale bar = 50 μm.

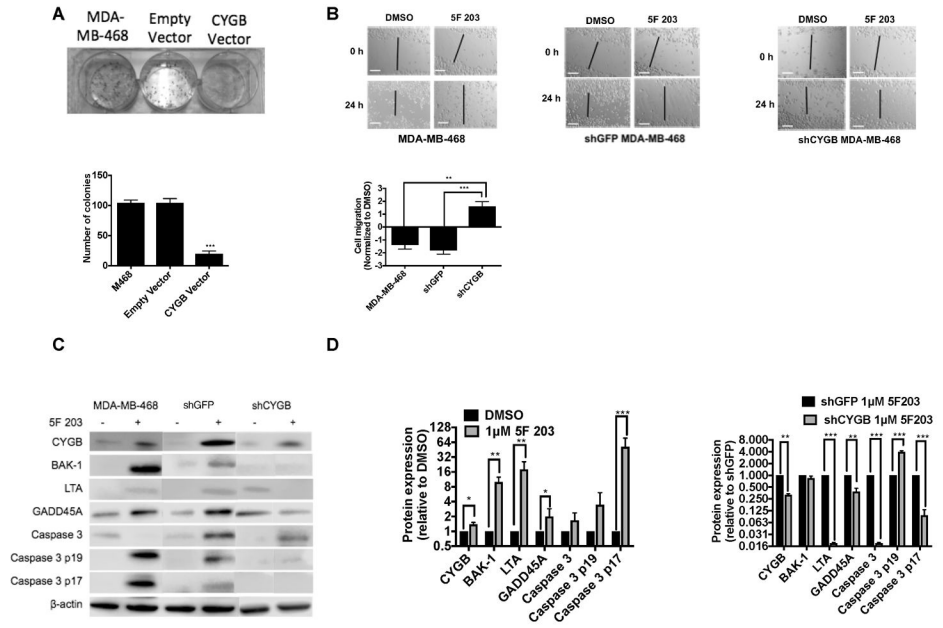

Figure 4. 5F 203 confers anticancer activity, induces CYGB and pro-apoptotic protein expression and produces caspase 3 cleavage in vitro.

(A) Colony formation analysis in MDA-MB-468 cells untransfected, transfected with empty vector or transfected to overexpress CYGB. Lower panel: quantification of colony numbers. (B) Assessment of migration in untransfected, shGFP and shCYGB MDA-MB-468 cells following 5F 203 treatment. Lower panel: wound closure, normalized to control. (C,D) Determination of CYGB, BAK-1, LTA and GADD45A protein expression as well as caspase 3 cleavage in untransfected, shGFP and shCYGB MDA-MB-468 cells following treatment with 5F 203 (1 μM, 72h). Scale bar = 100 μm. Bars, SEM. Statistically significant where indicated as designated * P< 0.05, **P < 0.01 or ***P < 0.001.

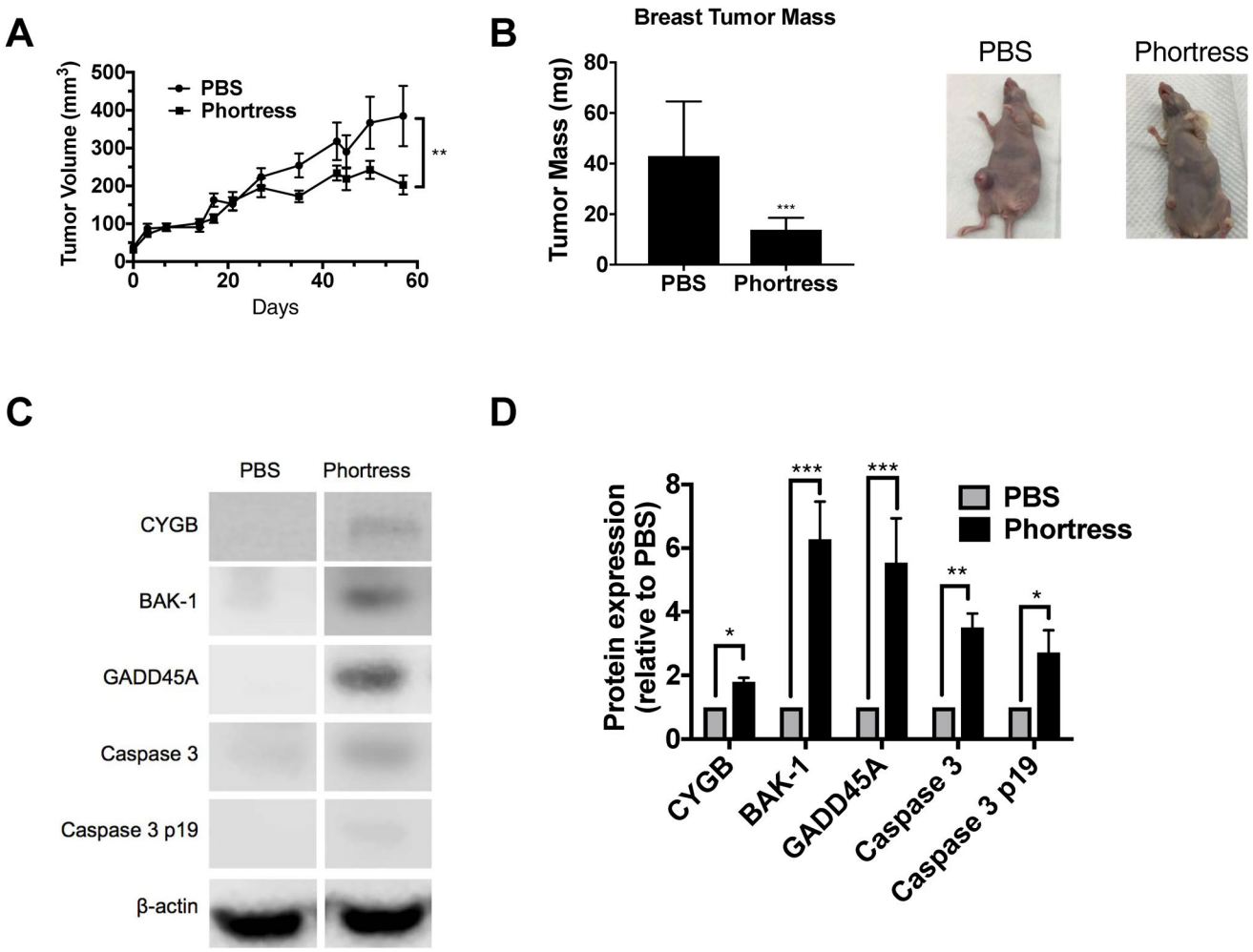

Figure 5. 5F 203 confers anticancer activity, induces CYGB and pro-apoptotic protein expression and produces caspase 3 cleavage in vivo.

(A,B) Effect of Phortress on tumor growth (as measured in tumor volume, N =11 and tumor mass, N = 9) for 3 cycles of 3 doses every other day (Q2D X 3) followed by a 10 d rest period as determined in Materials and Methods. (C,D) CYGB, BAK-1, and GADD45A protein expression as well as caspase 3 cleavage determination in tumor xenografts. N = 6. Bars, SEM. Statistically significant where indicated as designated * P< 0.05, **P < 0.01 or ***P < 0.001.

Table 1.

5F 203-mediated induction of genes that promote apoptosis in MDA-MB-468 cells

Symbol	Description	Function	Fold change
BAK-1	BCL2-antagonist/killer 1	Accelerates programmed cell death by binding to and antagonizing the anti-apoptotic action of BCL2 or its adenovirus homolog E18 19k protein.	3.9
LTA	Lymphotoxin alpha (TNF superfamily, member 1)	Lymphotoxin is produced by lymphocytes and cytotoxic for a wide range of tumor cells in vitro and in vivo.	5.5
GADD45a	Growth arrest and DNA damage-inducible alpha	Binds to proliferating cell nuclear antigen	3.5

Cells were exposed to 5F 203 (100 nM, 24h) before genes that regulate apoptosis were profiled using the RT^2 Profiler PCR array as described previously (McLean et al., 2015). Only genes induced greater than 3-fold are reported. Data represent the mean of two independent experiments performed in triplicate and are statistically significant at $p < 0.05$.